Decoupling CME Temporal Properties from Solar Cycle Effects And Analysis of Magnetic Field Evolution with Heliocentric Distance

Yakub Olufadi[1], Nada Al-Haddad[1], Noé Lugaz[1], Bin Zhuang[1], Charles Farrugia[1], Christian Moestl[2]

[1]University of New Hampshire [2]Austrian Space Weather Office

AGU25 New Orleans, LA | 15–19 December 2025

1. Introduction

Our previous study (Olufadi et al., 2025, in prep) and that of (Regnault et al., 2021) using CMEs measured at 1au have shown that nearly all CME properties vary with solar cycle (SC) activity, as illustrated in Figure [1]. We are currently conducting a more detailed analysis of the CME profile to differentiate the effects of the solar cycle from the inherent characteristics of the CMEs. For this study, we selected events near $\sim 1\ AU$ from over 1600 CME timestamps stored in the HELIO4CAST catalog (Möstl. et al., 2017).

Method: we adopt superposed epoch analysis (SEA) in this study.

SEA Result: Overall, B_{mag}, V_p and T_p enhanced profile in AP, indicate a stronger, hotter and more compressed sheath consistent with fast CME dynamics.

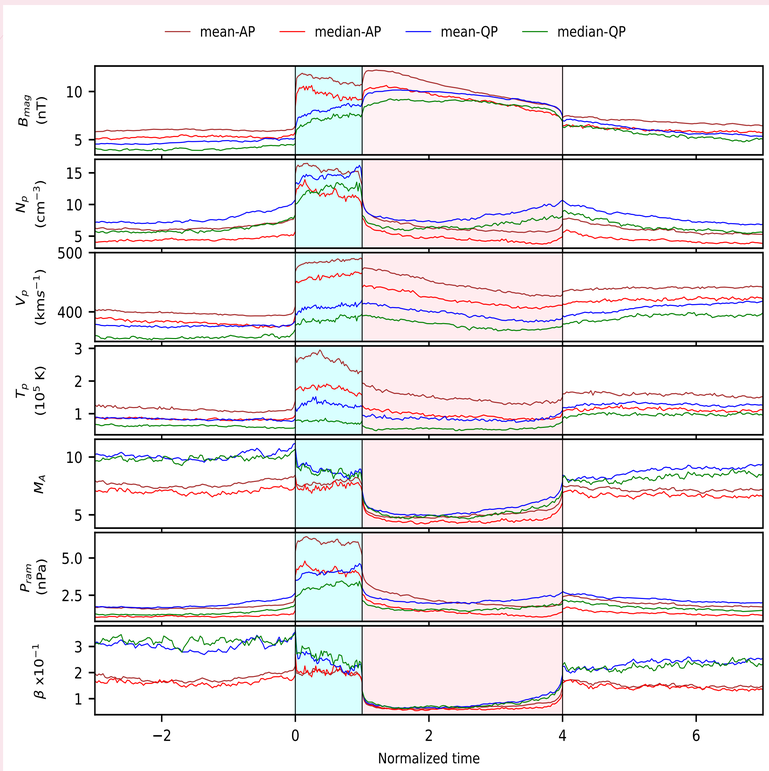

Figure 1. The combined SEA plot of AP and QP events.

2. SEA for Matching AP & QP Events

We construct a speed-matched subset of events, using similar ME velocities for both AP and QP CMEs, in order to eliminate the potential influence of CME speed when assessing the impact of solar-cycle activity on CME properties (for example, faster CMEs are found to have stronger magnetic field strength).

SEA Result: The close similarity in AP and QP profiles in figure 1 and 2 confirms that the temporal behaviors in Figure 1 are primarily driven by solar cycle variations, not CME speed.

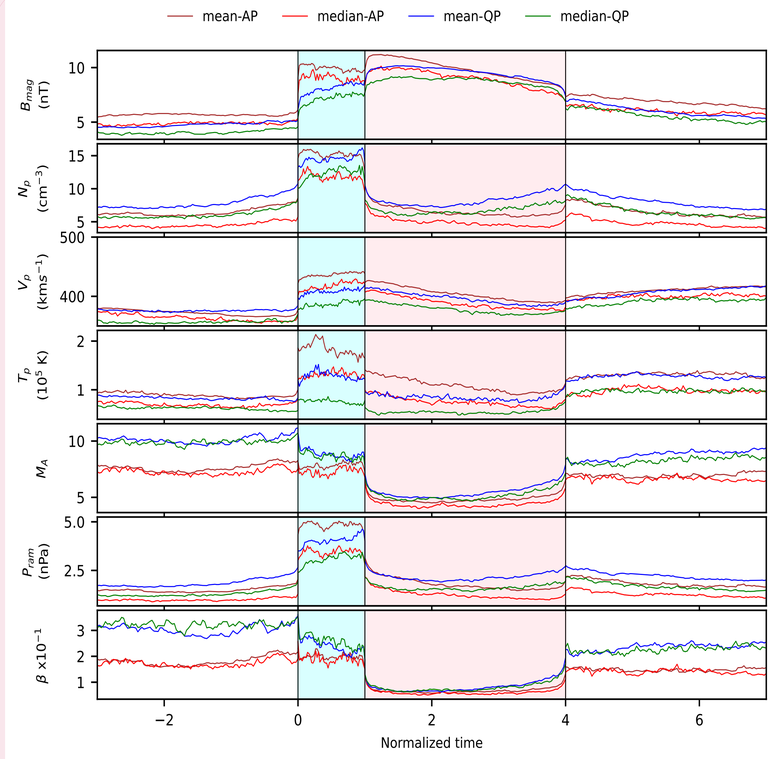

Figure 2. SEA for matching AP and QP events.

3. Heliocentric Distance Dependence

The variational study of CME features as a function of heliocentric distance. The figure below illustrates the geometry of a CME flux rope and its correspondence to the axes obtained from Minimum Variance Analysis (MVA). While MVA yields the minimum, intermediate, and maximum-variance directions of the magnetic field, these axes are commonly interpreted when the rotation is well defined as approximating the radial, poloidal, and axial directions of the flux-rope structure.

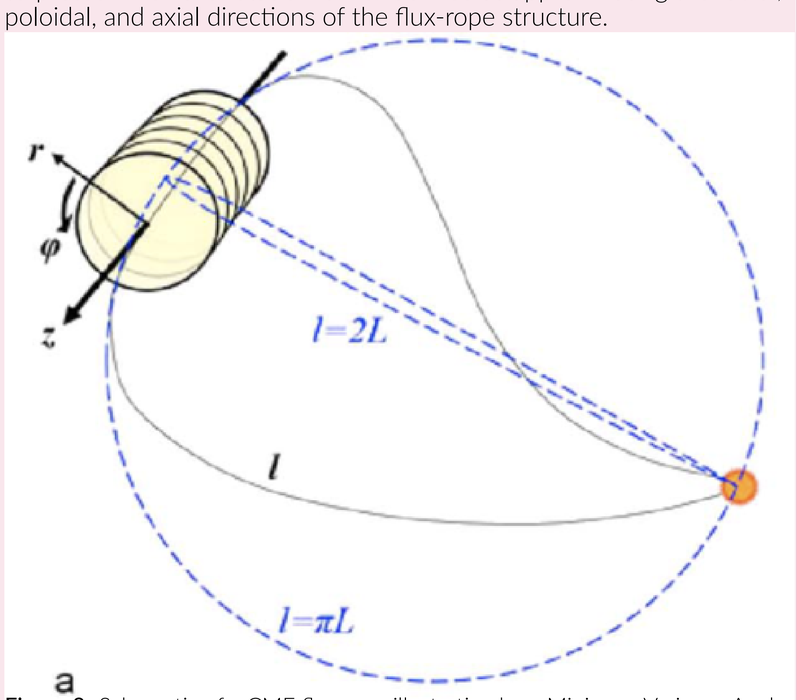

Figure 3. Schematic of a CME flux rope illustrating how Minimum Variance Analysis (Wang 2015)

We also study the variation in CME axial and poloidal magnetic field components derived using minimum variance analysis (MVA) as a function of heliocentric distance for all CME bins in this study.

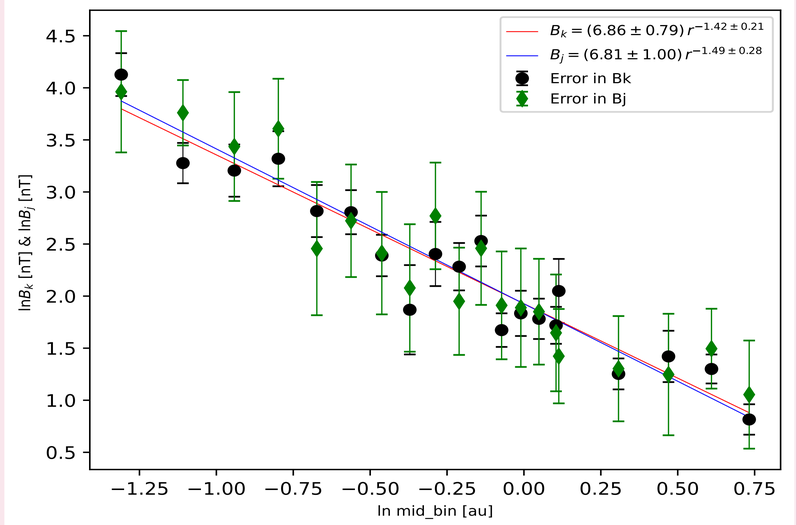

Figure 4. The plot of In max. B_k In max. B_j Vs. helio-dist. [In mid-bin]

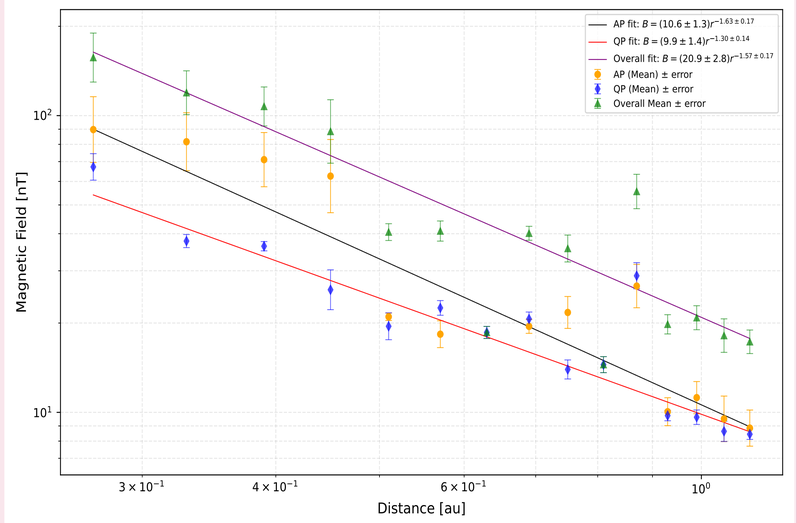

Figure 5. The Average Log-Log B-field Power Law Fitting Plot vs. helio-dist.

Still On Heliocentric Distance Dependence

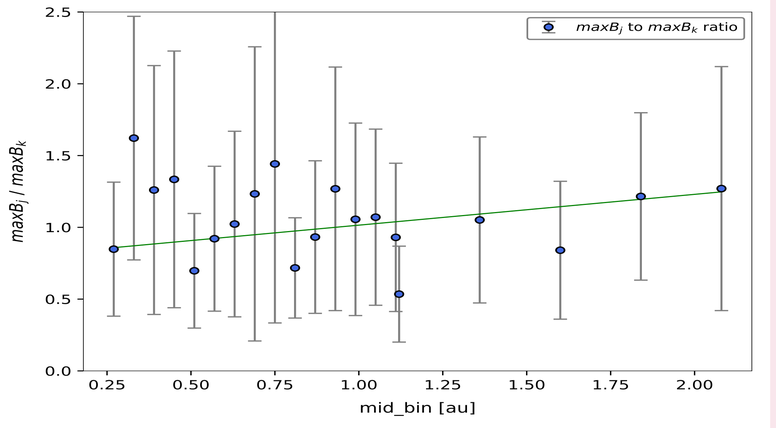

Figure 6. Sheath-ME ratio relative to heliocentric distance.

4. Ageing Effect

Here, we then investigate the aging effect of CMEs resulting from their expansion during propagation by examining the front-to-rear ratios of the Bk and Bj components, as well as the corresponding ratios within the sheath and ME regions.

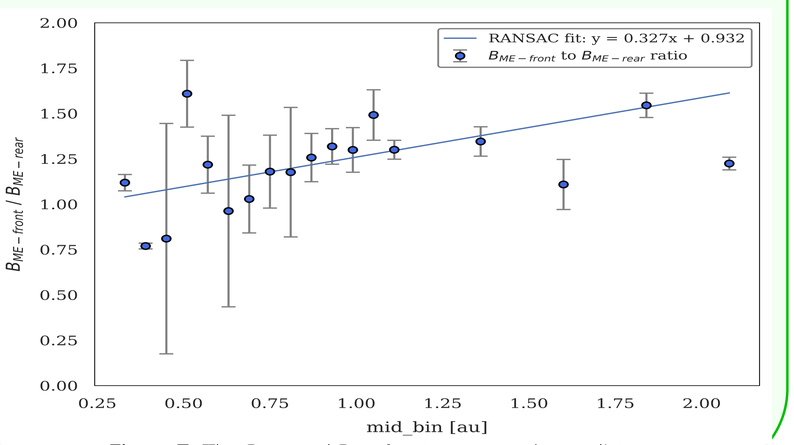

Figure 7. The B_{ME} and B_{SH} front to rear ratio vs. distance.

5. Result Summary

- Across all CME regions, AP events show enhanced B_{mag}, T_p, and V_p compared to QP events, while proton density n_p remains higher in QP. After applying a velocity-matching criterion to remove speed-related biases, the SEA profiles remain essentially unchanged, demonstrating that the AP–QP differences are intrinsic solar-cycle signatures rather than artifacts of CME propagation speed.
- At the ME front, proton temperature is consistently higher and more broadly distributed than at the rear, indicating a hotter leading region. The ME front also shows enhanced B_{mag} relative to the sheath, likely due to magnetic-field pileup or magnetic erosion, though distinguishing these effects requires further investigation.
- Similarly, RANSAC fits of the toroidal (B_k) and poloidal (B_j) components yield similar decay exponents (−1.42 and −1.49), within 15% of previous studies. This shows that B_k and B_j weaken at comparable rates, indicating self-similar expansion of CME magnetic fields.
- From Figure [5], the mean AP, QP, and overall CME $|\mathbf{B}|$ profiles all display clear power-law decay with heliocentric distance, with fitted exponents of -1.63, -1.30, and -1.57, respectively. These values are consistent with the $\sim r^{-1.5}$ behavior reported in Davies 2021, and minor deviations from the slopes presented in Wang 2005, Leitner 2007, and Winslow 2015 likely reflect differences in event selection, solar-cycle segmentation, and the extended multi-spacecraft distance range considered here.
- The front-to-rear ratios of ME B_{field} and B_j against B_k show no clear trend with distance, but most values are ≥ 1. This indicates systematically stronger fields at CME fronts, consistent with magnetic-field decay and aging as CMEs expand through the heliosphere.

6. References

Möstl., C., Isavnin., A., Boakes., P. D., et al. 2017, Space Weather, 15, 955

Olufadi, Y., Al-Haddad, N., Lugaz, N., et al. 2025, arXiv e-prints. `https://arxiv.org/abs/2506.xxxxx`

Regnault, F., Dasso, S., Auchere, F., et al. 2021, in 43rd COSPAR Scientific Assembly. Held 28 January - 4 February, Vol. 43, 1017

7. Acknowledgement

This research is being supported by NSF grant (AGS1954983), and NASA grants (80NSSC21K0463 & 80NSSC22K0349).

ybo1000@unh.edu